

Impaired function of inositol 1,4,5-trisphosphate receptor channels harboring disease-associated mutant subunits

Lara E. Terry, Kamil J. Alzayady, Sundeep Malik and David I. Yule

Supplementary Materials

Experimental Procedures

Measurement of ER Store Ca^{2+} content in Intact Cells

Table S1. Disease phenotypes of discussed IP₃R mutations in ligand binding domain, regulatory and coupling domain, and channel domain

Table S2. Molecular characteristics of disease associated IP₃R mutations in the ligand binding domain

Table S3. Molecular characteristics of disease associated IP₃R mutations in the regulatory and coupling domain

Table S4. Molecular characteristics of disease-associated IP₃R mutations in the c-terminal channel domain

Table S5. Mutagenesis primers

Table S6. Corresponding residues in the other sequences

Figure S1. Mutant IP₃R immunoprecipitated with wild-type IP₃R

Figure S2. Stable expression of IP₃R mutants tested do not alter ER Ca^{2+} store content

Figure S3. Mutant expression is increased in HEK-3KO cells compared to DT40-3KO cells

Figure S4. rIP₃R1ND and mIP₃R2^{GS} constructs localize to the ER membrane when stably expressed in HEK-3KO cells

Figure S5. rIP₃R1^{TI} is non-functional when expressed in HEK-3KO cells

Figure S6. rIP₃R1^{GR} is non-functional when expressed in HEK-3KO cells

Supplementary Materials:

Experimental Procedures

Measurement of ER Store Ca^{2+} content in Intact Cells

HEK cells were initially prepared as indicated above for population-based imaging of cytoplasmic Ca^{2+} ; however, prior to dispensing of cells in 96-well plate (~ 300,000 cells/well), cells were washed with and plated in a 0.1 mM Ca^{2+} imaging buffer. The plate was centrifuged at 200g for 2 minutes to plate cells to the bottom of each well. The plate rested for 30 min prior to commencing the assay. Fluorescence imaging was carried out using FlexStation 3 from Molecular Devices (excitation alternated between 340 nm and 380 nm and emission 510 nm). To force an extracellular Ca^{2+} concentration of 200nM, 0.1365 mM EGTA was added to the wells (calculated using MaxChelator). Subsequently, 30 μM CPA was added to block SERCA and allow for emptying of the ER Ca^{2+} store. Results were exported to Excel where ratio of 340/380 values and area under the curve were calculated. Data was averaged from 3 experimental runs.

| Mutation ^a | Original Residue (Base Change) & Reference Sequence ^b | | Isoform | Domain | Conserved ^c |
|-----------------------|--|-------------------------------|--|--------------------------------|-----------------------------|
| R269G | R269G (c.805C>G) in NM_001099952.2 | | <i>Itpr1</i> | Ligand Binding Domain | Yes |
| | Diagnosis | Individuals Affected | Reported Phenotype | | Reference |
| | SCA29 | 1 de novo case ^d | Infantile-onset non-progressive ataxia, hypotonia, gross motor delay and mild cognitive impairment | | Zambonin <i>et al.</i> 2017 |
| Mutation | Original Residue (Base Change) & Reference Sequence | | Isoform | Domain | Conserved |
| R269W | R269W (c.805C>T) in NM_001168272.1 & NM_001099952.2 | | <i>Itpr1</i> | Ligand Binding Domain | Yes |
| | Diagnosis | Individuals Affected | Reported Phenotype | | Reference |
| | Autosomal dominant NPCA | Mother & 2 Sons (inherited) | Infantile-onset cerebellar ataxia, cerebellar atrophy, delayed motor development, hypotonia, nystagmus, postural tremor, and slurred speech. Intellectual disability in one son. | | Barresi <i>et al.</i> 2016 |
| | SCA29 | 1 de novo case ^d | Infantile-onset non-progressive ataxia, hypotonia, gross motor delay and mild cognitive impairment | | Zambonin <i>et al.</i> 2017 |
| | Ataxic Cerebral Palsy | Mother & Daughter (inherited) | Infantile-onset cerebellar ataxia, intellectual disability, delayed motor development, cerebellar atrophy, myoclonic jerks, myokymia, postural tremor, hypotonia, and dysarthria | | Das <i>et al.</i> 2017 |
| | EOA | 2 de novo cases | <p><u>Case 1 (P2):</u> Non-progressive infantile onset ataxia, delayed motor development, mild cerebellar atrophy (vermis), isolated dyscalculia, slowing of horizontal saccades (COMA), convergent strabismus, and myoclonus in the extremities & trunk</p> <p><u>Case 2 (P6):</u> Non-progressive infantile onset ataxia, delayed motor development, nystagmus, hypotonia, mild cerebellar atrophy, cognitive impairment, & strabismus</p> | | Synofzik <i>et al.</i> 2018 |
| Mutation | Original Residue (Base Change) & Reference Sequence | | Isoform | Domain | Conserved |
| T594I | T594I (c.1781C>T) in NM_001099952.2 | | <i>Itpr1</i> | Regulatory and Coupling Domain | Yes |
| | Diagnosis | Individuals Affected | Reported Phenotype | | Reference |
| | Sporadic infantile-onset SCA | 1 Sporadic Case | Motor developmental delays, moderate cognitive deficits, ataxia, oculomotor apraxia, vertical and horizontal nystagmus observed as early as the first day of life, general hypotonia and postural tremor of the head, arms, and trunk, and diffuse cerebellar atrophy, as well as atrophy of the pontine tegmentum. No progressive motor or intellectual deterioration was observed during follow-up | | Sasaki <i>et al.</i> 2015 |
| Mutation | Original Residue (Base Change) & Reference Sequence | | Isoform | Domain | Conserved |
| N602D | N602D (c. 1804A>G) in NM_001099952.2 & (c.1759A>G) in NM_001168272.1 | | <i>Itpr1</i> | Regulatory and Coupling Domain | Yes |

| | Diagnosis | Individuals Affected | Reported Phenotype | | Reference |
|----------|---|---|--|--------------------|---|
| | Autosomal Dominant CNPCA/SCA29 | 4 Related Individuals (inherited) | <u>Proband</u> : Non-progressive ataxia, delayed gross motor development, cerebellar atrophy, cognitive delay, gaze-evoked nystagmus, epilepsy, hypotonia, truncal titubation, and limb ataxia <u>Father</u> : Delayed gross motor milestones, academic difficulties, saccadic eye movements with end range nystagmus, dysarthria, gait and limb ataxia, intension tremor, and diffuse cerebellar atrophy | | Huang <i>et al.</i> 2012 Zambonin <i>et al.</i> 2017 |
| | Ataxic Cerebral Palsy | 1 de novo case | Non-progressive ataxia, delayed gross motor development, moderate intellectual disability, hypotonia, and normal brain imaging | | Parolin Schneckenberg <i>et al.</i> 2015 |
| Mutation | Original Residue (Base Change) & Reference Sequence | | Isoform | Domain | Conserved |
| G2506R | G2506R (c.7516G>A) in NM_001099952.2 & G2539R (c.7615G>A/C) in NM_001168272.1 | | <i>Itpr1</i> | Selectivity Filter | Yes |
| | Diagnosis | Individuals Affected | Reported Phenotype | | Reference |
| | GS (c.7615G>A) | 5 de novo cases | <u>P261348</u> : Delayed ability to sit and walk independently, speech delay, mild learning difficulties, ataxia, hypotonia, bilateral iris hypoplasia, foveal hypoplasia, mild visual impairment, cerebellar hypoplasia/atrophy, gall stones, and scoliosis <u>P2021_2021</u> : Delayed ability to sit independently, moderate speech delay, mild to moderate learning difficulties, ataxia, hypotonia, bilateral iris hypoplasia, and cerebellar hypoplasia/atrophy <u>P2018_2018</u> : Ataxia, hypotonia, bilateral iris hypoplasia, and cerebellar hypoplasia/atrophy not known <u>P5284_5284</u> : Delayed ability to sit independently, speech delay, mild learning difficulties, ataxia, hypotonia, bilateral iris hypoplasia, mild visual impairment, cerebellar hypoplasia/atrophy, patent foramen ovale, and mild pulmonary valve stenosis <u>P5285_5285</u> : Moderate learning difficulties, ataxia, hypotonia, bilateral iris hypoplasia, and cerebellar hypoplasia/atrophy | | McEntagart <i>et al.</i> 2016 |
| | SCA29 ^d | 1 de novo case 1 inherited case | Infantile-onset non-progressive ataxia, hypotonia, gross motor delay and mild cognitive impairment | | Zambonin <i>et al.</i> 2017 |
| | GS (c.7615G>C) | 1 de novo case | Delayed ability to sit and walk independently, severe speech delay, learning difficulties, ataxia, bilateral iris hypoplasia, cerebellar hypoplasia/atrophy, and gastrointestinal reflux | | McEntagart <i>et al.</i> 2016 |
| Mutation | Original Residue (Base Change) & Reference Sequence | | Isoform | Domain | Conserved |
| G2498S | G2498S (c.7492G>A) in NM_002223.2 | | <i>Itpr2</i> | Selectivity Filter | Yes |
| | Diagnosis | Individuals Affected | Reported Phenotype | | Reference |
| | Anhidrosis | 5 Homozygous cases & 5 Heterozygous cases (inherited) | <u>Homozygous Individuals</u> : Anhidrosis with severe heat intolerance leading to increased heart rate and skin and ear canal temperatures <u>Heterozygous Individuals</u> : Asymptomatic | | Klar <i>et al.</i> 2014 |

Table S1. Disease phenotypes of discussed IP₃R mutations in ligand binding domain, regulatory and coupling domain, and channel domain.

Abbreviations: CNPCA: Congenital non-progressive cerebellar ataxia; EOA: early onset ataxia; GS: Gillespie Syndrome; NPCA: non-progressive congenital ataxia; SCA: Spinocerebellar Ataxia.

^a Mutations reported in the reference sequence of NP_001093422 (IP₃R1), NP_002214 (IP₃R2), or NP_002215 (IP₃R3). If not originally reported in this reference sequence, multiple sequence alignment was utilized to find residue in appropriate reference sequence.

^b This indicates the residue, base change, and reference sequence in which the mutation was originally discovered.

^c This refers to whether residue is conserved among human, rat, and mouse sequences of all three IP₃R isoforms.

^d Details of individuals phenotype beyond general SCA29 symptoms not provided.

| Mutation ^a | Original Residue (Base Change) & Reference Sequence ^b | Isoform | Domain | Conserved ^c | Diagnosis | Individuals Affected | Reference |
|-------------------------|--|--------------|--------|------------------------|------------------------------|------------------------------------|--|
| R241K | R241K (c.722G>A) in NM_001168272.1 | <i>Itpr1</i> | LBD | Yes | Autosomal dominant NPCA | Mother & Daughter (inherited) | Barresi <i>et al.</i> 2016 |
| E246K | E246K (c.736G>A) in NM_001099952.2 | <i>Itpr1</i> | LBD | Yes | EOA | 1 de novo case (Validation Cohort) | Synofzik <i>et al.</i> 2018 |
| T267M | T267M (c.800C>T) in NM_001099952.2 | <i>Itpr1</i> | LBD | Yes | Sporadic infantile-onset SCA | 1 Sporadic Case | Ohba <i>et al.</i> 2013 Sasaki <i>et al.</i> 2015 |
| | | | | | SCA29 | 2 Sporadic Cases | Zambonin <i>et al.</i> 2017 |
| | | | | | EOA | 1 de novo case (Validation Cohort) | Synofzik <i>et al.</i> 2018 |
| T267R | T267R (c.800C>G) in NM_001099952.2 | <i>Itpr1</i> | LBD | Yes | Sporadic infantile-onset SCA | 1 Sporadic Case | Sasaki <i>et al.</i> 2015 |
| R269G | R269G (c.805C>G) in NM_001099952.2 | <i>Itpr1</i> | LBD | Yes | SCA29 | 1 de novo case | Zambonin <i>et al.</i> 2017 |
| R269W | R269W (c.805C>T) in NM_001168272.1 & NM_001099952.2 | <i>Itpr1</i> | LBD | Yes | Autosomal dominant NPCA | Mother & 2 Sons (inherited) | Barresi <i>et al.</i> 2016 |
| | | | | | SCA29 | 1 de novo case | Zambonin <i>et al.</i> 2017 |
| | | | | | Ataxic Cerebral Palsy | Mother & Daughter (inherited) | Das <i>et al.</i> 2017 |
| | | | | | EOA | 2 de novo case (Validation Cohort) | Synofzik <i>et al.</i> 2018 |
| S277I | S277I (c.830G>T) in NM_001099952.2 | <i>Itpr1</i> | LBD | Yes | SCA15 (with early onset) | 1 Sporadic Case | Fogel <i>et al.</i> 2014 |
| | | | | | Sporadic infantile-onset SCA | 1 Sporadic Case | Sasaki <i>et al.</i> 2015 |
| | | | | | SCA29 | 1 de novo case | Zambonin <i>et al.</i> 2017 |
| K279E | K279E (c.835A>G) in NM_001099952.2 | <i>Itpr1</i> | LBD | No | SCA29 | 1 de novo case | Zambonin <i>et al.</i> 2017 |
| A280D | A280D (c.839C>A) in NM_001168272.1 | <i>Itpr1</i> | LBD | Yes | Autosomal dominant NPCA | 1 de novo case | Barresi <i>et al.</i> 2016 |
| Exon 14 Splice Mutation | Exon 14 (c.1207-2A-T) in <i>itpr1</i> | <i>Itpr1</i> | LBD | Yes | Autosomal dominant CNPCA | 4 Related Individuals (inherited) | Wang <i>et al.</i> 2017 |
| K417_418Ins | K417_418Ins (c.1252-1G>T) in NM_001099952.2 | <i>Itpr1</i> | LBD | No | SCA29 | 1 de novo case | Zambonin <i>et al.</i> 2017 |
| V494I | V494I (c.1480G>A) on NG_016144.1 | <i>Itpr1</i> | LBD | Yes | SCA15 | 1 Individual | Ganesamoorthy <i>et al.</i> 2009 |
| E512K | E497K (c.1889G>A) in NM_001168272.1 | <i>Itpr1</i> | LBD | No | Autosomal dominant NPCA | 1 de novo case | Barresi <i>et al.</i> 2016 |

| | | | | | | | |
|-------|-------------------------------------|--------------|-----|-----|-----|---|-----------------------------|
| R568G | R568G (c.1702A>G) in NM_001099952.2 | <i>Itpr1</i> | LBD | Yes | EOA | 1 de novo case (Also inherited M1144V & A2069S) | Synofzik <i>et al.</i> 2018 |
|-------|-------------------------------------|--------------|-----|-----|-----|---|-----------------------------|

Table S2. Molecular characteristics of disease associated IP₃R mutations in the ligand binding domain. Abbreviations: CNPCA: Congenital non-progressive cerebellar ataxia; EOA: early onset ataxia; LBD: Ligand Binding Domain; NPCA: non-progressive congenital ataxia; SCA: Spinocerebellar Ataxia.

^a Mutations reported in the reference sequence of NP_001093422 (IP₃R1), NP_002214 (IP₃R2), or NP_002215 (IP₃R3). If not originally reported in this reference sequence, multiple sequence alignment was utilized to find residue in appropriate reference sequence.

^b This indicates the residue, base change, and reference sequence in which the mutation was originally discovered.

^c This refers to whether residue is conserved among human, rat, and mouse sequences of all three IP₃R isoforms.

| Mutation ^a | Original Residue (Base Change) & Reference Sequence ^b | Isoform | Domain | Conserved ^c | Diagnosis | Individuals Affected | Reference |
|-----------------------|--|--------------|--------|------------------------|--------------------------------|---|---|
| T594I | T594I (c.1781C>T) in NM_001099952.2 | <i>Itpr1</i> | R/C | Yes | Sporadic infantile-onset SCA | 1 Sporadic Case | Sasaki <i>et al.</i> 2015 |
| N602D | N602D (c. 1804A>G) in NM_001099952.2 & (c.1759A>G) in NM_001168272.1 | <i>Itpr1</i> | R/C | Yes | Autosomal Dominant CNPCA/SCA29 | 4 Related Individuals (inherited) | Huang <i>et al.</i> 2012 Zambonin <i>et al.</i> 2017 |
| | | | | | Ataxic Cerebral Palsy | 1 de novo case | Parolin Schnekenberg <i>et al.</i> 2015 |
| R728* | R728* (c.2182C>T) in NM_001099952.2 | <i>Itpr1</i> | R/C | No | GS | 1 de novo case | Gerber <i>et al.</i> 2016 |
| A911V | A911V (c. 2732C>T) in NM_001099952.2 | <i>Itpr1</i> | R/C | No | EOA | 1 inherited case (Non-ataxic parents) | Synofzik <i>et al.</i> 2018 |
| | | | | | Hereditary Spastic Paraplegia | 7 Individuals in 2 Unrelated Families | Eler-Dobkowska <i>et al.</i> 2019 |
| N984fs | N984fs (c.2952_2953insTATA) in NM_001099952.2 | <i>Itpr1</i> | R/C | No | GS + Cardiovascular Symptoms | 2 Siblings | Carvalho <i>et al.</i> 2017 |
| P1074L | P1059L (c.8581C>T) in NM_002222.5 | <i>Itpr1</i> | R/C | No | SCA15 | Multiple Individuals (inherited) | Hara <i>et al.</i> 2008 |
| M1064V | M1064V (c.3190A>G) in NM_002224.3 | <i>Itpr3</i> | R/C | Yes | Neuropathy | 1 de novo case | Lassuthova <i>et al.</i> 2016 |
| M1144V | M1144V (c.3430A>G) in NM_001099952.2 | <i>Itpr1</i> | R/C | No | EOA | 1 inherited case (Also de novo R568G & inherited A2069S) | Synofzik <i>et al.</i> 2018 |
| | | | | | Hereditary Spastic Paraplegia | 1 case - inherited vs de novo unknown (A2069S also present) | Eler-Dobkowska <i>et al.</i> 2019 |
| T1386M | T1386M (c.4157C>T) in NM_001099952.2 | <i>Itpr1</i> | R/C | No | SCA29 | 1 de novo case | Zambonin <i>et al.</i> 2017 |
| T1424M | T1424M (c.4271C>T) in NM_002224.3 | <i>Itpr3</i> | R/C | Yes | Neuropathy | 1 de novo case | Schabhuttl <i>et al.</i> 2014 |
| S1493D | S1487D(c.4459_4460delinsGA) in NM_001168272.1 | <i>Itpr1</i> | R/C | Yes | Ataxic Cerebral Palsy | 1 de novo case | Parolin Schnekenberg <i>et al.</i> 2015 |
| V1553M | V1553M (c.4657G>A) in NM_001099952.2 | <i>Itpr1</i> | R/C | No | Autosomal Dominant CNPCA/SCA29 | 20 Related Individuals (inherited) | Dudding <i>et al.</i> 2004 Huang <i>et al.</i> 2012 Zambonin <i>et al.</i> 2017 |
| | | | | | SCA29 | 5 Related Individuals (inherited) | Shadrina <i>et al.</i> 2016 |

| | | | | | | | |
|----------------------------|--|--------------|-----|-----|---|---|------------------------------------|
| Q1558* | Q1558* (c.4672C>T) in NM_001099952.2 | <i>Itpr1</i> | R/C | No | GS | 1 de novo case | Gerber <i>et al.</i> 2016 |
| E1666D | E1666D (c.4998A>C) in NM_001099952.2 | <i>Itpr1</i> | R/C | No | EOA | 1 inherited case (Non-ataxic parents) | Synofzik <i>et al.</i> 2018 |
| L1787P | L1827P (c.5360T>C) in P29994.2 | <i>Itpr1</i> | R/C | Yes | SCA29 (Autosomal recessive) | 6 Homozygous Cases & 5 Heterozygous Cases (inherited) | Klar <i>et al.</i> 2017 |
| D1839N | D1839N (c.5515G>A) in NP_002214.2 | <i>Itpr2</i> | R/C | No | FIHP | Mother & daughter | Cetani <i>et al.</i> 2019 |
| E2061G | E2094G (c.6281A>G) in NM_001168272.1 | <i>Itpr1</i> | R/C | Yes | GS | Mother & Daughter (inherited) | McEntagart <i>et al.</i> 2016 |
| E2061Q | E2094Q (c.6280G>C) in NM_001168272.1 | <i>Itpr1</i> | R/C | Yes | GS | 1 de novo case | McEntagart <i>et al.</i> 2016 |
| E2061K | E2094K (c.6280G>A) | <i>Itpr1</i> | R/C | Yes | GS with minor cerebellar involvement & no intellectual disability | 1 de novo case | Stendel <i>et al.</i> 2019 |
| A2069S | A2069S (c.6205G>T) in NM_001099952.2 | <i>Itpr1</i> | R/C | Yes | EOA | 1 inherited case (Also de novo R568G & inherited M1144V) | Synofzik <i>et al.</i> 2018 |
| | | | | | Hereditary Spastic Paraplegia | 1 case - inherited vs de novo unknown (M1144V also present) | Elert-Dobkowska <i>et al.</i> 2019 |
| G2102Valfs5*/A2221Valfs23* | G2102Valfs5*/A2221Valfs23* (c.6366+3A>T/c.6664+5G>T) in NM_001099952.2 | <i>Itpr1</i> | R/C | No | GS | 1 de novo case | Gerber <i>et al.</i> 2016 |

Table S3. Molecular characteristics of disease associated IP₃R mutations in the regulatory and coupling domain.

Abbreviations: CNPCA: Congenital non-progressive cerebellar ataxia; EOA: early onset ataxia; FIHP: Familial Isolated Primary Hyperparathyroidism; GS: Gillespie Syndrome; R/C: Regulatory and Coupling Domain; SCA: Spinocerebellar Ataxia.

^a Mutations reported in the reference sequence of NP_001093422 (IP₃R1), NP_002214 (IP₃R2), or NP_002215 (IP₃R3). If not originally reported in this reference sequence, multiple sequence alignment was utilized to find residue in appropriate reference sequence.

^b This indicates the residue, base change, and reference sequence in which the mutation was originally discovered.

^c This refers to whether residue is conserved among human, rat, and mouse sequences of all three IP₃R isoforms.

| Mutation ^a | Original Residue (Base Change) & Reference Sequence ^b | Isoform | Domain | Conserved ^c | Diagnosis | Individuals Affected | Reference |
|-----------------------|--|--------------|---|------------------------|--|---|--|
| L2403P | L2403P (c.7208T>C) in NM_001099952.2 | <i>Itpr1</i> | 1 st -4 th TM Domains | Yes | EOA | 1 de novo case | Synofzik <i>et al.</i> 2018 |
| S2454F | S2439F ^d | <i>Itpr1</i> | 5 th -6 th TM Domains | No | SS | 1 Individual | Prasad <i>et al.</i> 2016 |
| T2490M | T2523M (c.7568C>T) ^e | <i>Itpr1</i> | 5 th -6 th TM Domains | Yes | Unassigned SCA (Progressive optic atrophy, ataxia, etc.) | 1 Individual | Valencia <i>et al.</i> 2015 |
| G2506R | G2506R (c.7516G>A) in NM_001099952.2 & G2539R (c.7615G>A/C) in NM_001168272.1 | <i>Itpr1</i> | Selectivity Filter | Yes | GS (c.7615G>A) | 5 de novo cases | McEntagart <i>et al.</i> 2016 |
| | | | | | SCA29 | 1 de novo case 1 inherited case | Zambonin <i>et al.</i> 2017 |
| | | | | | GS (c.7615G>C) | 1 de novo case | McEntagart <i>et al.</i> 2016 |
| G2498S | G2498S (c.7492G>A) in NM_002223.2 | <i>Itpr2</i> | Selectivity Filter | Yes | Anhidrosis | 5 Homozygous cases & 5 Heterozygous cases (inherited) | Klar <i>et al.</i> 2014 |
| S2508L | S2508L (chr12:26553068G>A) | <i>Itpr2</i> | TM | No | SS | 1 Individual | Prasad <i>et al.</i> 2016 |
| V2541A | V2574A (c.7721T>C) in NM_001168272 | <i>Itpr1</i> | 6 th TM Domain | Yes | Molecularly unassigned SCA | Mother & Daughter (inherited) | Hsiao <i>et al.</i> 2017 |
| N2543I | N2576I (c.7727A>T) in NM_001168272.1 | <i>Itpr1</i> | 6 th TM Domain | Yes | GS | 1 de novo case | Dentici <i>et al.</i> 2017 |
| G2547A | G2547A (chr3:4856819G>C) | <i>Itpr1</i> | 6 th TM Domain | Yes | SCA29 | 1 de novo case | Gonzaga-Jauregui <i>et al.</i> 2015 |
| I2550N | I2550N (c.7649T>A) in NM_001099952.2 | <i>Itpr1</i> | 6 th TM Domain | Yes | PCH | 1 de novo case | Van Dijk <i>et al.</i> 2016 |
| I2550T | I2550T (c.7649T>C) in NM_001099952.2 | <i>Itpr1</i> | 6 th TM Domain | Yes | SCA29 | 2 sporadic individuals | Zambonin <i>et al.</i> 2017 |
| T2552P | T2585P (c.7753C>A) in NM_001168272.1 | <i>Itpr1</i> | 6 th TM Domain | Yes | MICPCH | 1 de novo case | Hayashi <i>et al.</i> 2017 |
| F2553L | F2553L (c.7659T>G) in NM_001099952.2 | <i>Itpr1</i> | 6 th TM Domain | Yes | GS | 1 de novo case | Gerber <i>et al.</i> 2016 |
| K2563del. | K2563del. in NM_001099952.2 K2596del. (c.7786_7788delAAG) in NM_001168272.1 | <i>Itpr1</i> | LNK Domain | Yes | GS | 4 de novo cases | McEntagart <i>et al.</i> 2016 Gerber <i>et al.</i> 2016 |
| | | | | | SCA29 with Aniridia | 1 de novo individual | Zambonin <i>et al.</i> 2017 |
| | | | | | GS | 1 de novo case | Dentici <i>et al.</i> 2017 |
| | | | | | EOA w/Aniridia | 1 de novo case | Synofzik <i>et al.</i> 2018 |

| | | | | | | | |
|--|--|--|--|--|----|----------------|-----------------------------|
| | | | | | GS | 1 de novo case | de Silva <i>et al.</i> 2018 |
|--|--|--|--|--|----|----------------|-----------------------------|

Table S4. Molecular characteristics of disease-associated IP₃R mutations in the c-terminal channel domain.

Abbreviations: EOA: early onset ataxia; GS: Gillespie Syndrome; LNK: Linker Domain; MICPCH: microcephaly with pontine and cerebellar hypoplasia; PCH: pontocerebellar hypoplasia; SCA: Spinocerebellar Ataxia; SS: Sézary Syndrome; TM: Transmembrane.

^a Mutations reported in the reference sequence of NP_001093422 (IP₃R1), NP_002214 (IP₃R2), or NP_002215 (IP₃R3). If not originally reported in this reference sequence, multiple sequence alignment was utilized to find residue in appropriate reference sequence.

^b This indicates the residue, base change, and reference sequence in which the mutation was originally discovered.

^c This refers to whether residue is conserved among human, rat, and mouse sequences of all three IP₃R isoforms.

^d Residue was originally reported as S2439F in *itpr1* without reference sequence. Assumption was made that reference sequence was human (NP_002213.5).

^e Reference sequence of residue was not reported. Based on multiple sequence alignment, reference sequence was assumed to be in NM_001168272.1 based on appropriate amino acid residue present.

| | Primer Name | Primer | Silent Mutation Introduced |
|------------------|--|--|-----------------------------------|
| Primer 1 | R269W rIP ₃ R1 Forward | GCAGCACGTCTTCCTACGTACAACCGGCTGGCAGTCAGCCACGTCCG | SNaBI |
| Primer 2 | R269W rIP ₃ R1 Reverse | CGACGTGGCTGACTGCCAGCCGGTTGTACGTAGGAAGACGTGCTGC | SNaBI |
| Primer 3 | R269W hIP ₃ R1 Forward | CAGCACGTCTTCCTACGTACCACGGGCTGGCAGTCGGCCACATCTGCC | SNaBI |
| Primer 4 | R269W hIP ₃ R1 Reverse | GGCAGATGTGGCCGACTGCCAGCCCGTGGTACGTAGGAAGACGTGCTG | SNaBI |
| Primer 5 | N602D rIP ₃ R1 Forward | GCCCTGCTCCACAACGATCGAAAGCTCCTG | Pvul |
| Primer 6 | N602D rIP ₃ R1 Reverse | CAGGAGCTTTCGATCGTTGTGGAGCAGGGC | Pvul |
| Primer 7 | T594I hIP ₃ R1 Forward | GATGTGTTGGCTGAAGATATCATCACTGCCCTGCTCC | EcoRV |
| Primer 8 | T594I hIP ₃ R1 Reverse | GGAGCAGGGCAGTGATGATATCTTCAGCCAACACATC | EcoRV |
| Primer 9 | G2506R (G>A) hIP ₃ R1 Forward | GAGTCACGGGCTACGTAGCAGGGGTGGAGTAGGAGATG | SNaBI |
| Primer 10 | G2506R (G>A) hIP ₃ R1 Reverse | CATCTCCTACTCCACCCCTGCTACGTAGCCCGTGACTC | SNaBI |
| Primer 11 | G2506R (G>C) hIP ₃ R1 Forward | GAGTCACGGGCTACGTAGCCGGGGTGGAGTAGGAG | SNaBI |
| Primer 12 | G2506R (G>C) hIP ₃ R1 Reverse | CTCCTACTCCACCCCGGCTACGTAGCCCGTGACTC | SNaBI |
| Primer 13 | G2498S mIP ₃ R2 Forward | GGCCTCAGGAATGGATCCGGAGTTGGGGATGTGCTG | BamHI |
| Primer 14 | G2498S mIP ₃ R2 Reverse | CAGCACATCCCAACTCCGGATCCATTCCTGAGGCC | BamHI |

Table S5. Mutagenesis primers.

Primers used to introduce desired mutation and silently introduce restriction site.

| Residue of Interest | Arg269 | Thr594 | Asn602 | Gly2506 | Gly2498 |
|--|---------------------|---------------------|---------------------|------------------|---------------------|
| Original Sequence | <i>NP_001007236</i> | <i>NP_001093422</i> | <i>NP_001007236</i> | <i>NP_064307</i> | <i>NP_001093422</i> |
| NP_001093422 (hIP ₃ R1 variant 1) | 269 | 594 | 602 | 2506 | 2507 |
| NP_002213 (hIP ₃ R1 variant 2) | 269 | 579 | 587 | 2491 | 2492 |
| NP_001161744 (hIP ₃ R1 variant 3) | 269 | 579 | 587 | 2539 | 2540 |
| NP_001007236 (rIP ₃ R1 variant 1) | 269 | 594 | 602 | 2544 | 2545 |
| NP_001257525 (rIP ₃ R1 variant 2) | 269 | 579 | 587 | 2529 | 2530 |
| NP_001257526 (rIP ₃ R1 variant 3) | 269 | 594 | 602 | 2505 | 2506 |
| NP_034715 (mIP ₃ R1) | 269 | 594 | 602 | 2545 | 2546 |
| Q14643 (hIP ₃ R1 Structure) | 269 | 594 | 602 | 2546 | 2547 |
| P29994 (rIP ₃ R1 Structure) | 269 | 594 | 602 | 2554 | 2555 |
| NP_002214 (hIP ₃ R2) | 269 | 594 | 602 | 2497 | 2498 |
| NP_112308 (rIP ₃ R2) | 269 | 594 | 602 | 2497 | 2498 |
| NP_064307 (mIP ₃ R2 variant 1) | 269 | 594 | 602 | 2497 | 2498 |
| NP_34716 (mIP ₃ R2 variant 2) | 235 | 561 | 569 | 2464 | 2465 |
| NP_002215 (hIP ₃ R3) | 270 | 594 | 602 | 2473 | 2474 |
| NP_037270 (rIP ₃ R3) | 270 | 594 | 602 | 2472 | 2473 |
| NP_542120 (mIP ₃ R3) | 270 | 594 | 602 | 2472 | 2473 |

Table S6. Corresponding residues in the other commonly used IP₃R sequences. Residues of interest are referred to in the sequence indicated and the corresponding amino acid number is listed for other human, rat, and mouse sequences of all three IP₃R isoforms.

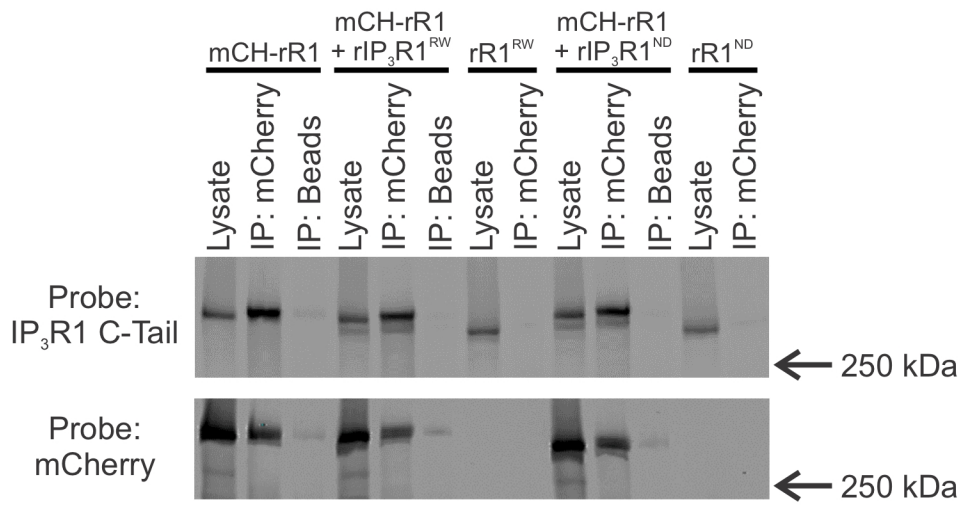
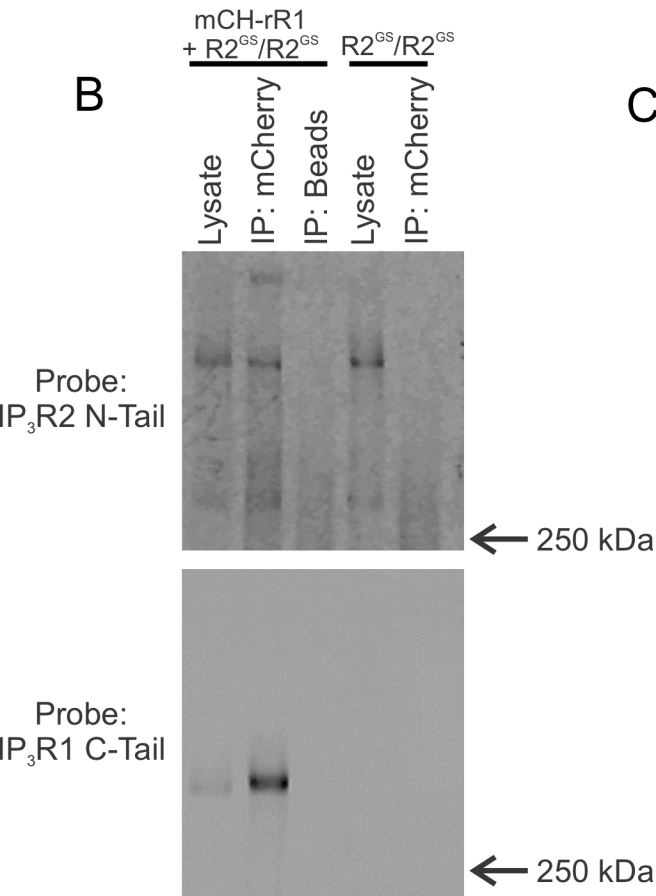
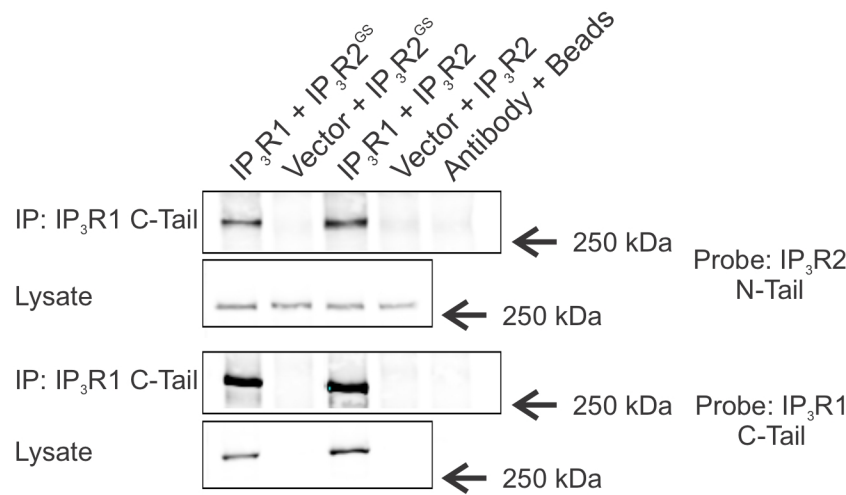
A**B****C**

Figure S1. Mutant IP₃R immunoprecipitated with wild-type IP₃R. **A.** mCherry tagged IP₃R1 was transiently co-transfected into HEK-3KO cells with or without rIP₃R1^{RW} and rIP₃R1ND. Pulldown with mCherry antibody resulted in co-immunoprecipitation of both rIP₃R1^{RW} and rIP₃R1ND when probed with c-terminal IP₃R1. **B.** R2^{GS}/R2^{GS} was transiently co-transfected into HEK-3KO cells with or without mCherry tagged IP₃R1. Pulldown with an antibody for mCherry resulted in co-immunoprecipitation of R2^{GS}/R2^{GS} when probed with n-terminal IP₃R2. **C.** WT mIP₃R2 and mIP₃R2^{GS} were transiently co-transfected into HEK-3KO cells with either rIP₃R1 or vector. Pulldown with α -c-terminal IP₃R1 resulted in co-immunoprecipitation of both WT mIP₃R2 and mIP₃R2^{GS} when probed with n-terminal IP₃R2.

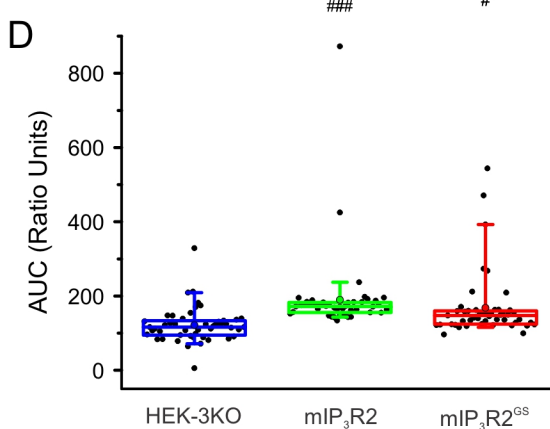
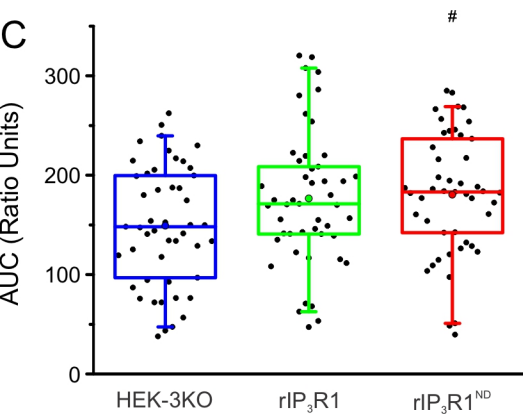
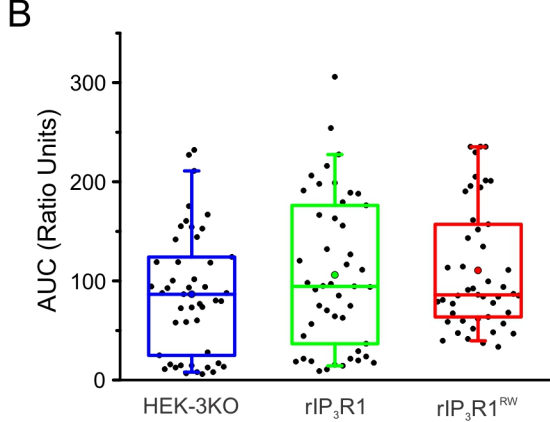
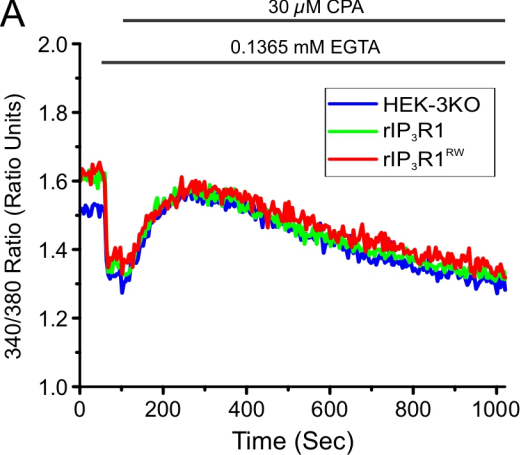


Figure S2. Stable expression of IP₃R mutants tested do not alter ER Ca²⁺ store content. **A.** HEK-3KO cells were loaded with Fura-2/AM and dispensed in a 96-well plate (~ 300,000 cells/well) in Ca²⁺ free imaging buffer. Fluorescence imaging was carried out using FlexStation 3 from Molecular Devices (excitation alternated between 340 nm and 380 nm and emission 510 nm). To force an extracellular Ca²⁺ concentration of 200nM, 0.1365 mM EGTA was added to the wells. Subsequently, 30 μM CPA was added to block SERCA and allow for emptying of the ER Ca²⁺ store. Results were exported to Excel where ratio of 340/380 values and area under the curve were calculated. **B.** Scatter plots summarizing Ca²⁺ content of ER store (area under the curve) for stable HEK-3KO cell lines expressing rIP₃R1^{RW}. Experiments were performed as shown in A. Boxes represent the 25th, 50th, and 75th percentiles, while whiskers represent 5th and 95th percentiles and mean is represented by colored circle. **C.** Scatter plots summarizing Ca²⁺ content of ER store (area under the curve) for stable HEK-3KO cell lines expressing rIP₃R1ND. Experiments were performed as shown in A. Boxes represent the 25th, 50th, and 75th percentiles, while whiskers represent 5th and 95th percentiles and mean is represented by colored circle. **D.** Scatter plots summarizing Ca²⁺ content of ER store (area under the curve) for stable HEK-3KO cell lines expressing mIP₃R2^{GS}. Experiments were performed as shown in A. Boxes represent the 25th, 50th, and 75th percentiles, while whiskers represent 5th and 95th percentiles and mean is represented by colored circle. Unless otherwise stated, all data above comes from at least N=3 experiments. #*P* < 0.05 and ###*P* < 0.001 when compared to HEK-3KO cell line; one-way ANOVA with Tukey's test was performed in B ($F_{2,91} = 1.630, p < 0.2017$), C ($F_{2,140} = 3.408, p < 0.0359$), and D ($F_{2,141} = 8.002, p < 0.0005$).

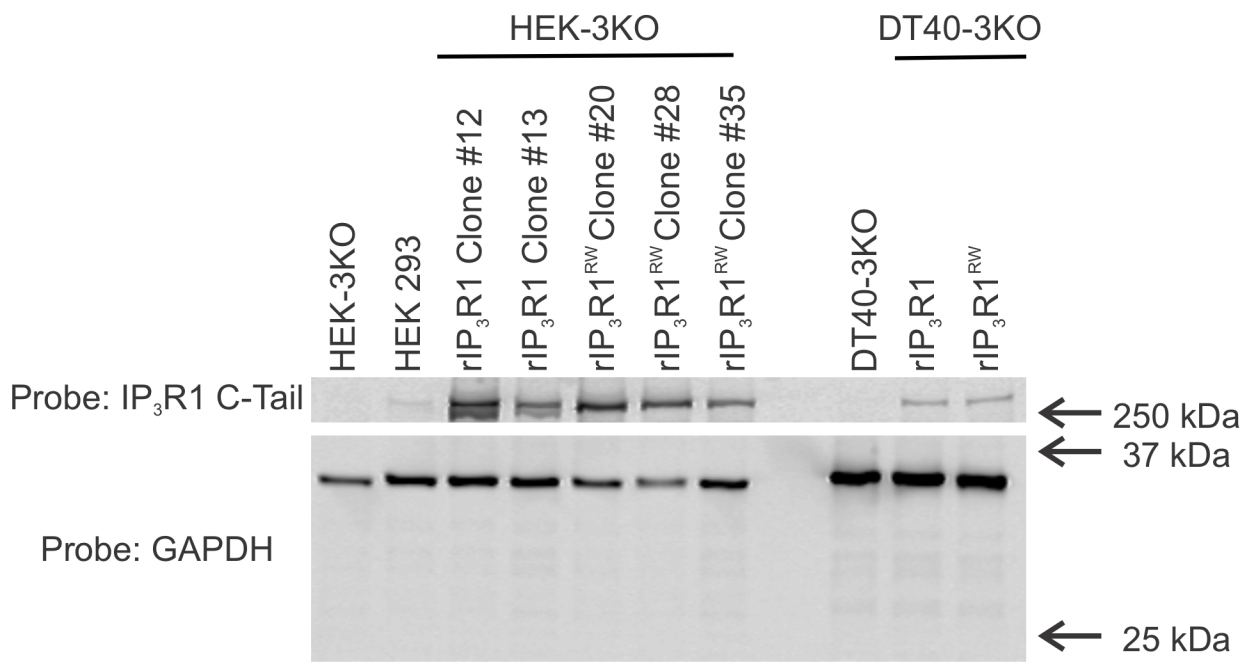
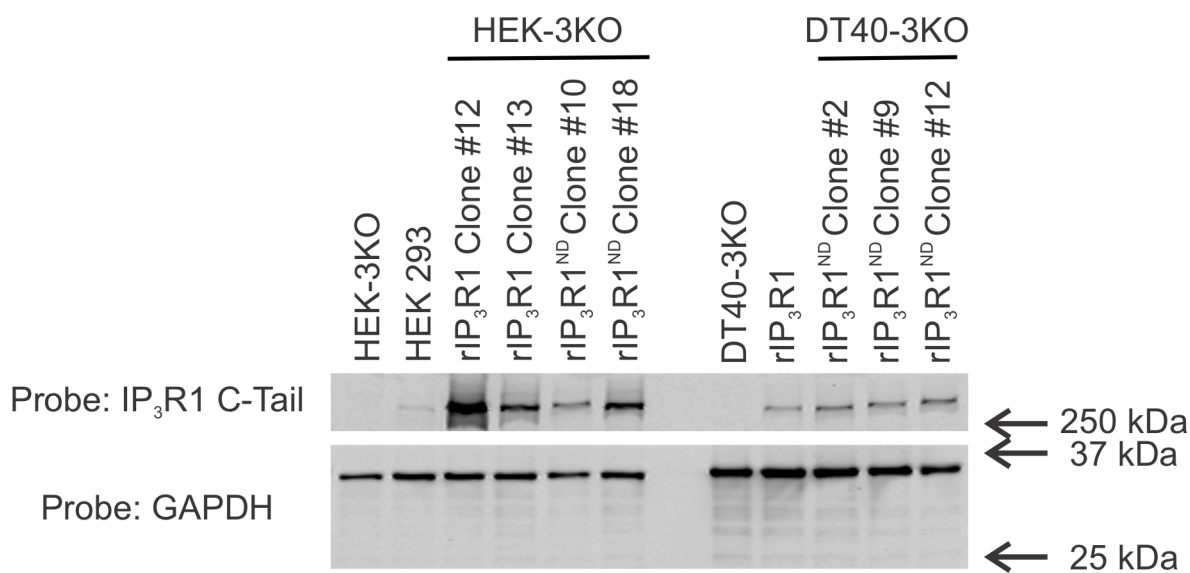
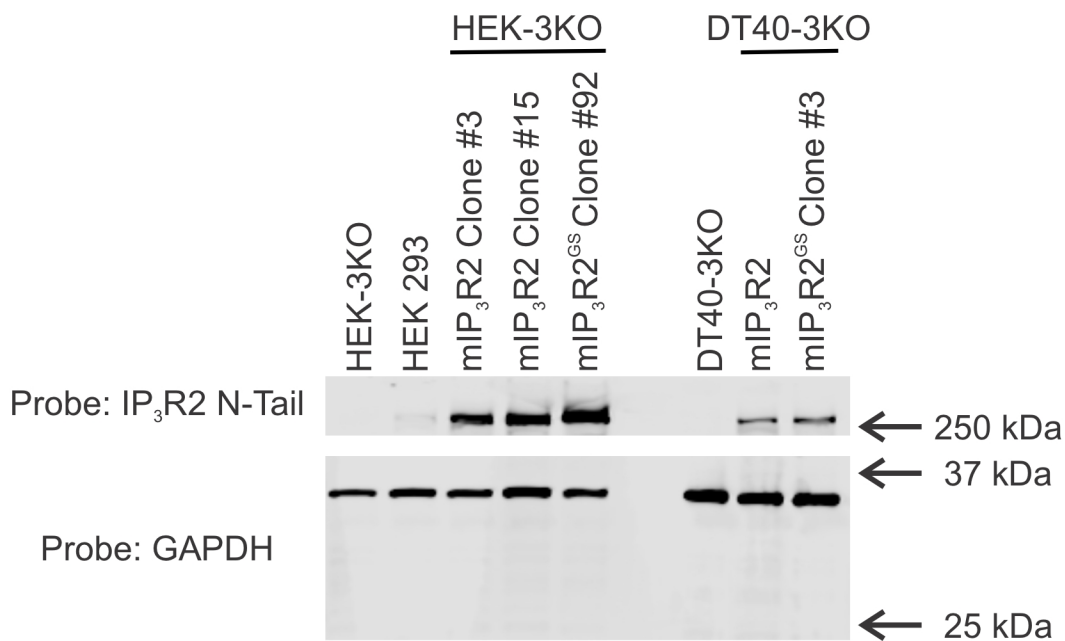
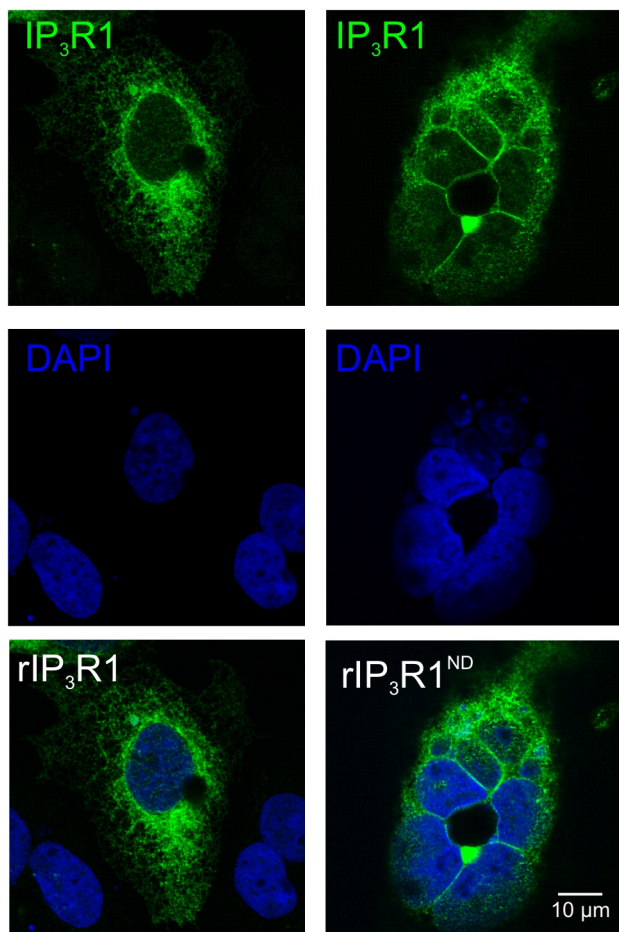
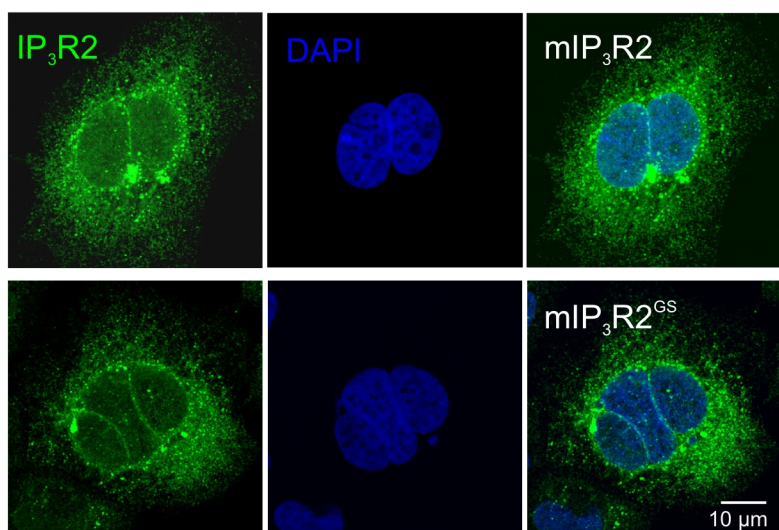
A**B****C**

Figure S3. Mutant expression is increased in HEK-3KO cells compared to DT40-3KO cells. **A.** WT rIP₃R1 and mutant rIP₃R1^{RW} cell lines were generated in the IP₃R-null HEK-3KO cells and DT40-3KO cells and western blotted for c-terminal IP₃R1 and GAPDH. **B.** WT rIP₃R1 and mutant rIP₃R1ND cell lines were generated in the IP₃R-null HEK-3KO cells and DT40-3KO cells and western blotted for c-terminal IP₃R1 and GAPDH. **C.** WT mIP₃R2 and mutant mIP₃R2^{GS} cell lines were generated in the IP₃R-null HEK-3KO cells and DT40-3KO cells and western blotted for n-terminal IP₃R2 and GAPDH.

A



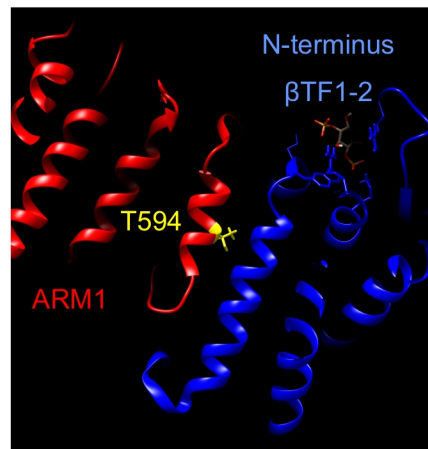
B



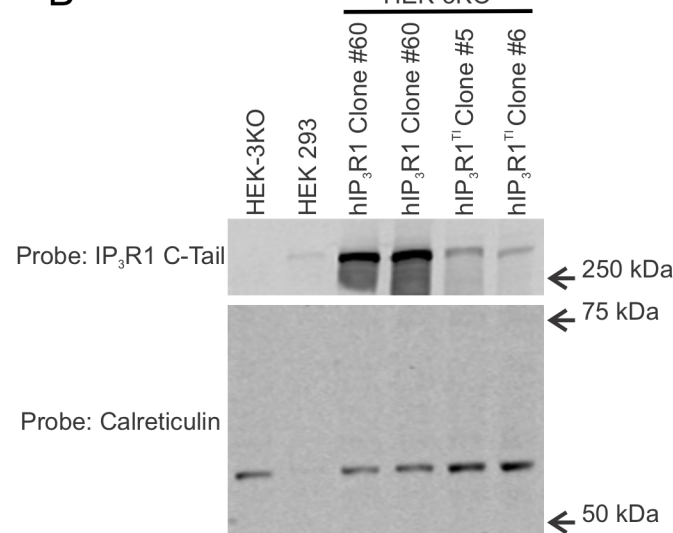
S4

Figure S4. rIP₃R1ND and mIP₃R2^{GS} constructs localize to the ER membrane when stably expressed in HEK-3KO cells. **A.** Immunocytochemistry for HEK-3KO cell lines expressing either WT rIP₃R1 (left) or mutant rIP₃R1ND (right). Top, IP₃R1 detection (green); middle, DAPI detection (blue); bottom, merged images of IP₃R1 and DAPI. Scale bars, 10 μm. **B.** Immunocytochemistry for HEK-3KO cell lines expressing either WT mIP₃R2 (top) or mutant mIP₃R2^{GS} (bottom). Left, IP₃R2 detection (green); middle, DAPI detection (blue); right, merged images of IP₃R2 and DAPI. Scale bars, 10 μm.

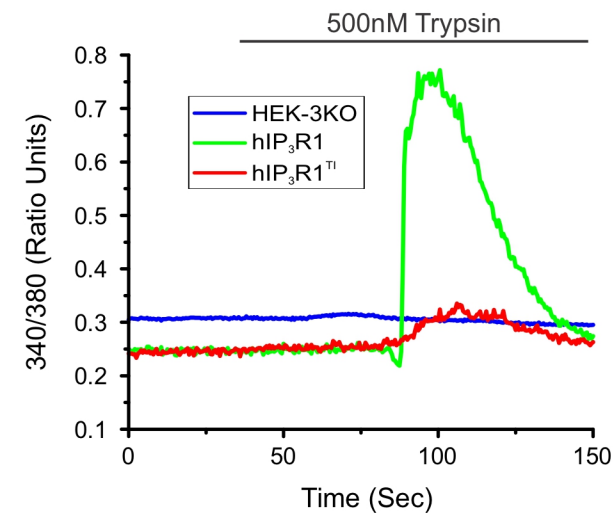
A



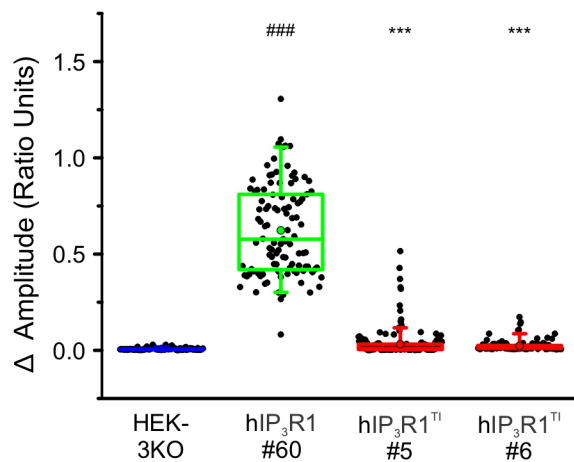
B



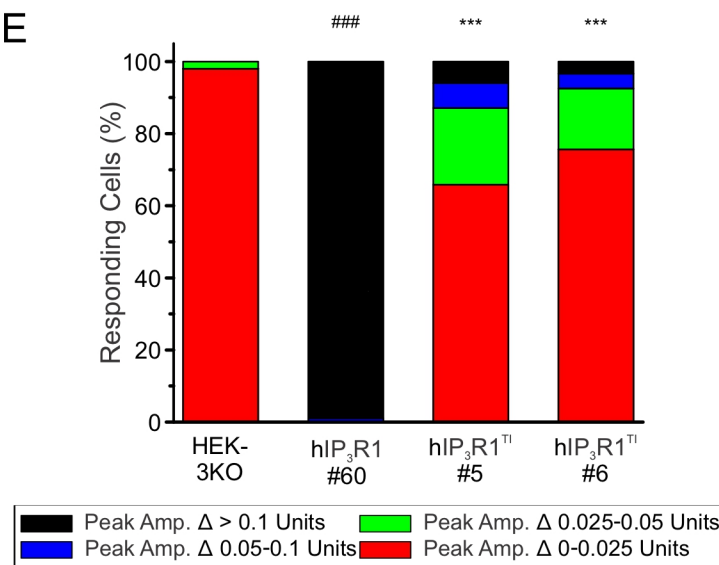
C



D



E



F

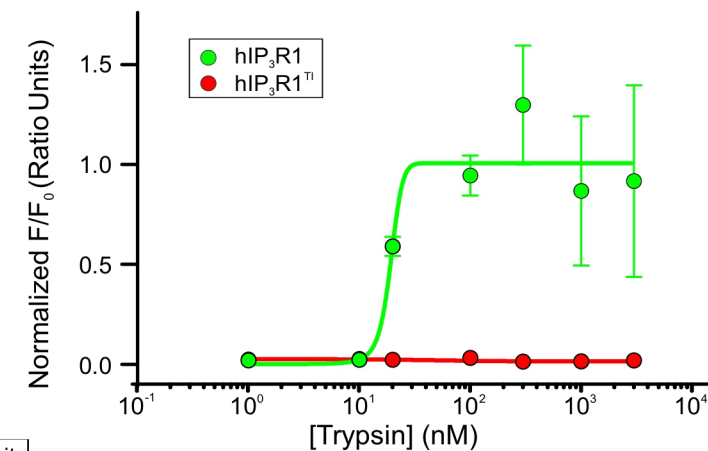


Figure S5. rIP₃R^{TI} is poorly functional when expressed in HEK-3KO cells. **A.** Chimera (PDB: 6DQN) was used to visualize WT Thr594 (yellow) located near the junction of the ARM1 domain (red) and the β-TF1 and β-TF2 domains of the LBD in the N-terminus (blue). **B.** WT hIP₃R1 and multiple mutant hIP₃R^{TI} cell lines generated in the IP₃R-null HEK-3KO cells were western blotted. **C.** Representative traces show Ca²⁺ signals of IP₃R-null HEK-3KO cells (blue), WT hIP₃R1 (green), and hIP₃R^{TI} (red) in response to trypsin (500 nM) when loaded with Fura-2/AM. **D.** Scatter plots summarizing change in amplitude (Peak ratio – Basal ratio: average of initial 5 ratio points) for experiments similar to those shown in B when treated with 500 nM trypsin. Boxes represent the 25th, 50th, and 75th percentiles, while whiskers represent 5th and 95th percentiles and mean is represented by colored circle. **E.** Stacked bar graph summarizing the percentage of amplitudes from D which fall into pre-determined ranges such that only those cells with an amplitude change greater than 0.1 ratio units (black portion of bars) are considered to be responding to the trypsin stimulus shown in C. **F.** Dose-response curve showing Ca²⁺ response of Fura-2/AM loaded WT hIP₃R1 and hIP₃R^{TI} cells when treated with increasing concentrations (1 nM, 10 nM, 30 nM, 100 nM, 300 nM, 1 μM, and 3 μM) of trypsin using a Flexstation3 96-well plate reader. Data are mean ± SEM of three (N = 3) independent experiments. ****P* < 0.001 when compared to WT rIP₃R1 cell line and ###*P* < 0.001 when compared to HEK-3KO cell line; one-way ANOVA with Tukey's test was performed in D ($F_{3,530} = 784.8$, *p* < 0.0001) and E ($F_{3,10} = 298.7$, *p* < 0.0001). Unless otherwise stated, all data above comes from at least N=3 experiments.

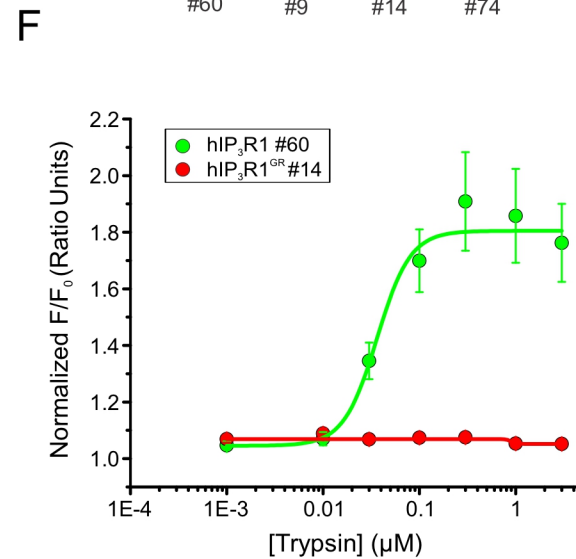
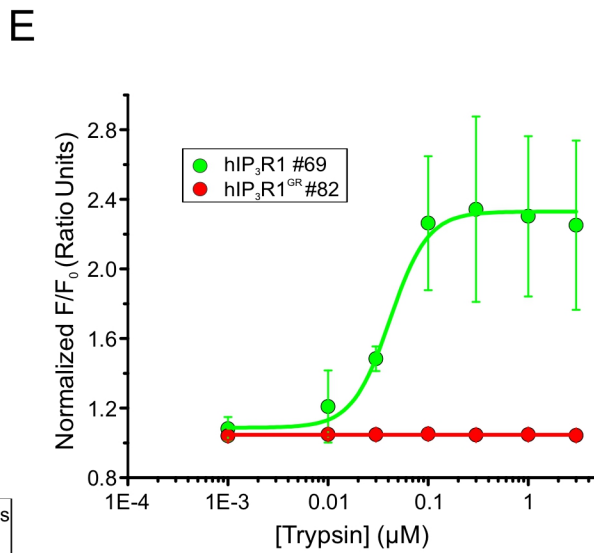
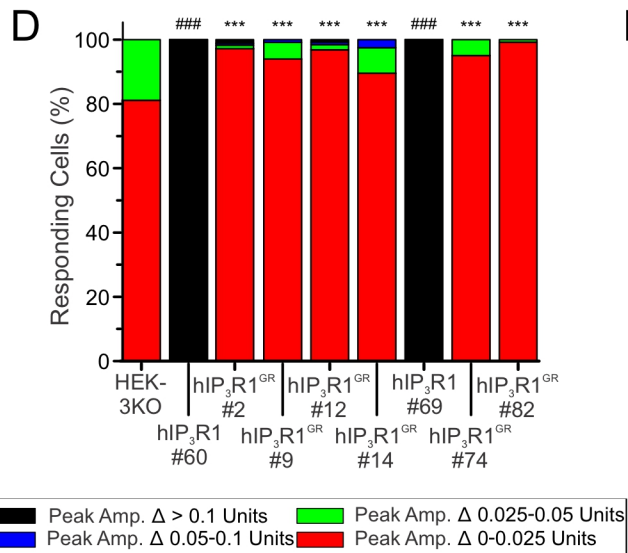
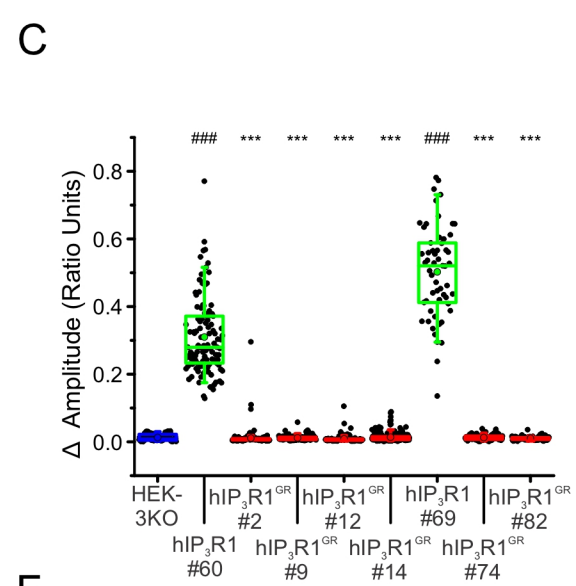
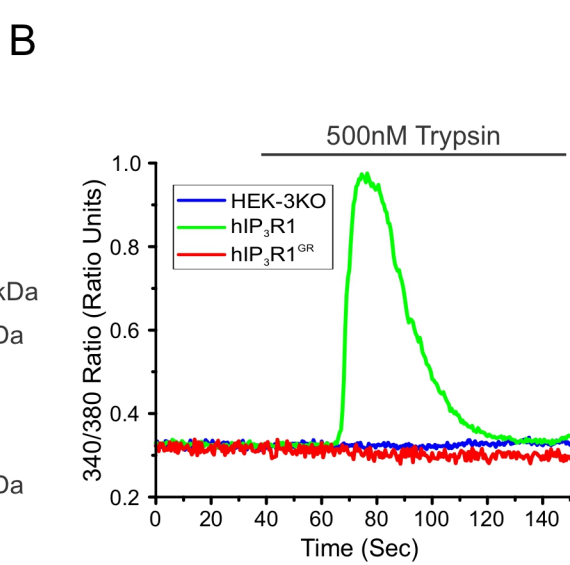
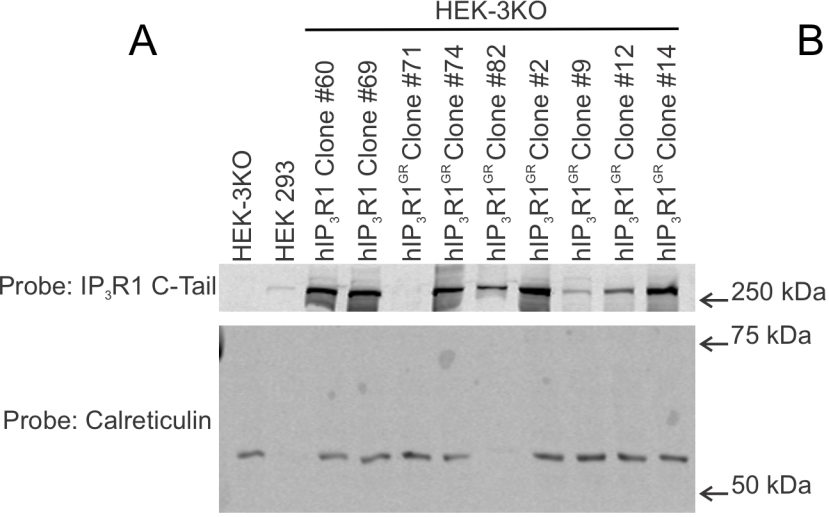


Figure S6. hIP₃R1^{GR} is non-functional when expressed in HEK-3KO cells. **A.** Multiple WT hIP₃R1 and mutant hIP₃R1^{GR} cell lines were generated in the IP₃R-null HEK-3KO cells and western blotted. hIP₃R1^{GR} cell lines #2, #9, #12, and #14 contain the GGG to CGG mutation made using primers 9 and 10 (Table S5), while hIP₃R1^{GR} cell lines #74 and #82 contain the GGG to AGG mutation made using primers 7 and 8 (Table S5). **B.** Representative traces show Ca²⁺ signals of IP₃R-null HEK-3KO cells (blue), WT hIP₃R1 (green), and hIP₃R1^{GR} (red) in response to trypsin (500 nM) when loaded with Fura-2/AM. **C.** Scatter plots summarizing change in amplitude (Peak ratio – Basal ratio: average of initial 5 ratio points) for experiments similar to those shown in B when treated with 5 nM, 50nM, and 500 nM of trypsin. Boxes represent the 25th, 50th, and 75th percentiles, while whiskers represent 5th and 95th percentiles and mean is represented by colored circle. **D.** Stacked bar graph summarizing the percentage of amplitudes from C which fall into pre-determined ranges such that only those cells with an amplitude change greater than 0.1 ratio units (black portion of bars) are considered to be responding to the trypsin stimulus shown in B. **E.** Dose-response curve showing Ca²⁺ response of Fura-2/AM loaded WT hIP₃R1 cell line #60 and hIP₃R1^{GR} cell line #14 when treated with increasing concentrations (1 nM, 10 nM, 30 nM, 100 nM, 300 nM, 1 μM, and 3 μM) of trypsin using a Flexstation3 96-well plate reader. Data are mean ± SEM of three (N = 3) independent experiments. **F.** Dose-response curve showing Ca²⁺ response of Fura-2/AM loaded WT hIP₃R1 cell line #69 and hIP₃R1^{GR} cell line #82 when treated with increasing concentrations (1 nM, 10 nM, 30 nM, 100 nM, 300 nM, 1 μM, and 3 μM) of trypsin using a Flexstation3 96-well plate reader. Data are mean ± SEM of three (N = 3) independent experiments. ****P* < 0.001 when compared to WT hIP₃R1 cell line and ###*P* < 0.001 when compared to HEK-3KO cell line; one-way ANOVA with Tukey's test was performed in C ($F_{8,1264} = 1245$, $p < 0.0001$) and D ($F_{8,28} = 16203$, $p < 0.0001$). Unless otherwise stated, all data above comes from at least N=3 experiments.